

Copper Vapor Catalyzing Role in the Growth of Graphene

Yuan Chang^{a§}, Shiji Li^{a§}, Tianyu He^a, Hongsheng Liu^a, Junfeng Gao^{a,b*}

^a *State Key Laboratory of Structural Analysis for Industrial Equipment, Dalian University of Technology, Dalian, 116024, China*

^b *Suzhou Laboratory, Suzhou, 215123, China*

*Email: gaojf@dlut.edu.cn

§ Y. C. and S. L. contributed equally to this work

Abstract: Cu is most used substrate to grow monolayer graphene under a temperature near melting point. In this study, we elaborated a remarkable amount of Cu clusters were continuously evaporated during the graphene growth, resulting into the vapor pressure comparable with the CH₄. Importantly, the decomposition barrier of CH₄ on Cu clusters is similar or even lower than on Cu surface. CuCH₄ serves as the primary active cluster in complex intermediates, exhibiting a growth-promoting effect. Particularly after the first graphene layer coverage, it may emerge as a dominant catalytic factor for multilayer growth by supplying critical growth species. Through controlled seed incorporation, this mechanism is expected to enable large-area controllable growth of bilayer and multilayer graphene structures.

Key Words: Cu vapor; Cluster; Graphene; Growth

Graphene is a standout material, widely used in various applications including seawater desalination, wearable devices, heat dissipation films, transparent touchscreens, ultra-sensitive sensors, biomedical diagnostics and therapy, and nano-drug delivery. Chemical vapor deposition (CVD) enables the bottom-up growth of graphene with large-area and precise controllability¹⁻³, which has emerged as the preferred method for scaled-up production. Graphene production via CVD relies on carbon-containing precursor like methane (CH₄) and catalytic substrate like Copper (Cu) due to its ability to facilitate dehydrogenation of hydrocarbon. The weak interaction and low carbon solubility of Cu enable direct single-layer graphene formation on its surface and exhibit self-limiting effect at low pressure⁴.

Notably, Cu substrate can be evaporated and form Cu clusters vapor under the growth temperature near Cu melting points. Small clusters are usually very active and have excellent catalysis capacity in chemistry^{5,6}. We can expect that the Cu clusters in vapor are also active for C precursors (CH₄) in the CVD process. Using Cu foam⁷ and Cu-containing carbon sources⁸ ensures a continuous supply of Cu vapor, promoting ultra-clean single-layer graphene growth. Pre-depositing Cu allows graphene formation on inert SiO₂ substrate⁹. These initial efforts confirm the existence of non-negligible Cu clusters vapor and their important role in the CVD growth of graphene.

However, the role of Cu clusters in vapor is still quite unclear. What are the real structure and population of Cu clusters? How they interact with precursors? Can Cu clusters in vapor help the dehydrogenation of CH₄ and promote the graphene? What is the kinetics of CH₄ catalyzing by Cu clusters in vapor and their impact on gas-phase equilibrium? So many puzzles were poorly understood, and accurate comprehensive atomic simulations is urgent to unveil the underlying mechanisms.

In this letter, we systematically explored the conditions, structure, stability, kinetics, and role of Cu vapor in graphene growth during CH₄ decomposition using first-principles calculations. We first examined the adsorption-desorption behavior of Cu vapor by comparing chemical potentials and adsorption energies. The derived pressure-temperature (P-T) conditions align with most previous experiments, confirming the widespread presence of Cu vapor in the CVD environment for graphene growth. Cu₁₋₄ clusters, which account for 99% of all Cu clusters, exhibit catalytic activity comparable

to, or even surpassing, Cu substrate surfaces in the initial CH₄ dehydrogenation. We identified the most stable CuCH₄ cluster for complex gas-phase reactions. Our analysis suggests that surface-adsorbed CuCH₄ clusters tend to diffuse towards the edge of pre-provided graphene nucleus on the top layer. This behavior may represent a growth mechanism that occurs once the Cu substrate is fully covered by graphene. Therefore, the generation and behavior of Cu vapor are critical for controlling the CVD process.

The adsorption–desorption behavior can be described by comparing the chemical potential (μ) of ideal gas with its adsorption energy (E_{ads}). When E_{ads} is less than μ , net adsorption of atoms will continue, whereas desorption from substrate to vapor will occur when μ is less than E_{ads} . The μ for the ideal gas is defined as the following equations¹⁰:

$$\mu = -k_B T \ln(g k_B T / p \times \zeta_{trans} \zeta_{rot} \zeta_{vibr}) \quad (1)$$

$$\zeta_{trans} = (2\pi m k_B T / h^2)^{3/2} \quad (2)$$

$$\zeta_{rot} = (1/\pi\sigma) \{8\pi^3 (I_A I_B \dots)^{1/n} k_B T / h^2\}^{n/2} \quad (3)$$

$$\zeta_{vibr} = \prod_{i=1}^{3N-3} \{1 - e^{-h\nu_i/k_B T}\}^{-1} \quad (4)$$

where ζ_{trans} , ζ_{rot} and ζ_{vibr} are the partition function for the translational motion, the rotational motion and the vibrational motion, respectively. It is feasible to consider the Cu vapor as consisting of individual Cu atoms. This approach allows the complex vibrational entropy and rotational entropy to be disregarded. Subsequently, μ of Cu vapor, can be calculated:

$$\mu = -k_B T \ln(k_B T / p \times g (2\pi m k_B T / h^2)^{3/2}) \quad (5)$$

where $k_B = 1.381 \times 10^{-23} \text{ J/K}$ is the Boltzmann constant. T is gas temperature, p is beam equivalent pressure of particle, $g = 2$ is the degeneracy of electronic energy levels for Cu, $m = 1.063 \times 10^{-25} \text{ kg}$ is the mass of a particle, $h = 6.626 \times 10^{-34} \text{ eV} \cdot \text{s}$ is the Planck constant. It should be noted that actual vapor may contain Cu clusters, the total partial pressure of Cu vapor is higher than estimation.

Under equilibrium conditions, E_{ads} of Cu vapor is defined as the following equation:

$$E_{ads} = E_{sub+Cu} - E_{sub} - E_{isolate Cu} \quad (6)$$

where E_{sub+Cu} is the total energy of system, E_{sub} and $E_{isolate Cu}$ denote the energy of Cu substrate and isolate Cu atom in vacuum, respectively. The actual copper substrate may consist of multiple crystal facets. In this study, we tested the E_{ads} of Cu on different

crystallographic planes. As shown in Fig. 1(a), our calculations indicate E_{ads} of -3.382 eV for Cu(100), -3.746 eV for Cu(110) and -3.129 eV for Cu(111) surface. The adsorption sites had been carefully tested.

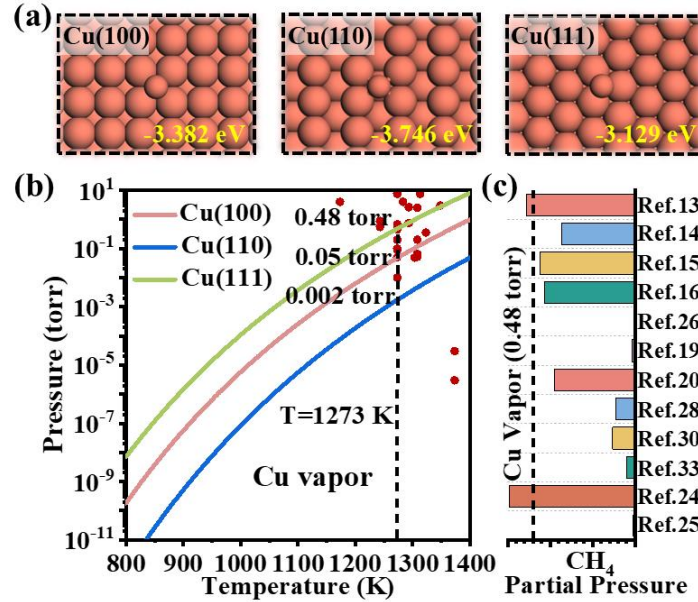


Fig. 1. (a) Adsorption energy of single Cu on common Cu surfaces. (b) The adsorption–desorption transition curve of Cu vapor. Red dots represent experimental P–T conditions ¹¹⁻³⁷. (c) Comparison of Cu vapor and experimental CH₄ partial pressure at 1273K.

The adsorption–desorption transition curve of Cu vapor were given in Fig. 1(b), with the equilibrium partial ranking from highest to lowest as Cu(111) > Cu(100) > Cu(110). This can be easily explained by the adsorption strength of Cu atoms on different surfaces, among which Cu(111) has the weakest adsorption on Cu atoms. The statistical analysis of existing low-pressure experimental data ¹¹⁻³⁷ (Red dots in Fig. 1(b)) indicates that most P–T conditions satisfy the desorption criteria proposed in this study. In the experimental investigation of Cu contamination, it is evident to the naked eye that the Cu deposition on the inner walls of quartz tube after CVD growth is remarkably far broader than the area of the substrate ^{38, 39}. These evidences confirm the prevalence of Cu vapor in graphene synthesis (see Sec. 1 of the Supplemental Material for more details). As shown in Fig. 1(c), the Cu vapor can reach 0.48 torr at 1273 K, which is comparable to the partial pressure of CH₄ under the same temperature, emphasizing its significance as a non-negligible factor.

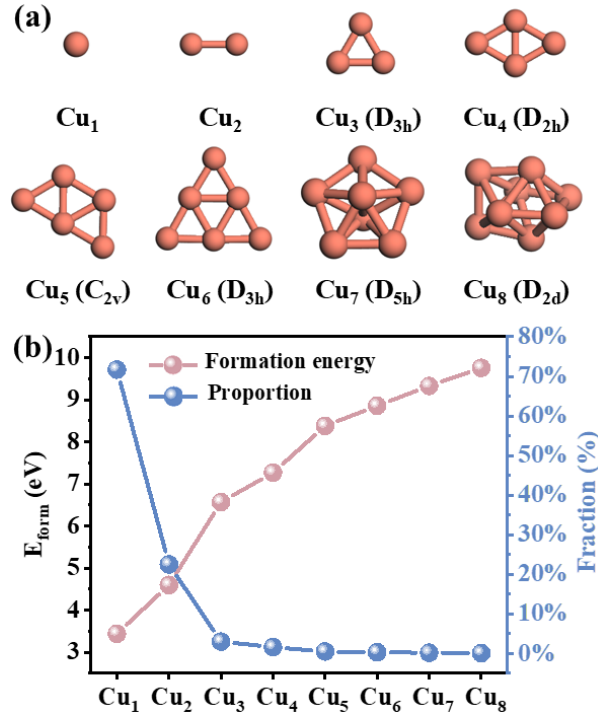


Fig. 2. (a) The ground state structures and (b) corresponding formation energy as well as proportion of Cu₁₋₈ clusters.

In the preceding discussion, Cu vapor was considered as individual atoms; however, in real growth conditions during graphene synthesis via CVD, collisions and aggregation of Cu atoms can occur. Therefore, determining the size of Cu clusters is essential before further research. The relative population of Cu clusters with different size can be estimated using the formula:

$$N \propto e^{-\Delta E/k_B T} \quad (7)$$

where ΔE is the relative energy difference of Cu cluster formation. To facilitate this analysis, the formation energy of Cu clusters was defined as:

$$E_{form} = E_{cluster} - N_{Cu} E_{Cu} \quad (8)$$

where $E_{cluster}$ represents the total energy of Cu cluster, E_{Cu} denotes the energy per Cu atom in its face-centered cubic bulk phase and N_{Cu} is the number of Cu atoms within the Cu cluster. As shown in Fig. 2, we had determined the ground state structures of Cu₁₋₈ clusters. The proportion of Cu₁₋₄ clusters has weighted 99%, while that of Cu₅₋₈ clusters has markedly reduced to less than 1% of the total content. This finding indicates a low probability of individual Cu atoms colliding and agglomerating into larger clusters in the

Cu vapor. Consequently, for the Cu cluster-catalyzed CH₄ dehydrogenation process being considered, the focus on Cu₁ to Cu₄ clusters is deemed adequate.

Due to the structural stability of CH₄ molecules, the initial step of dehydrogenation faces a challenging energy barrier⁴⁰. Nevertheless, a series of radical chain reactions will be initiated facilitated by C–H bond activation after this step, resulting in the significant production of carbon radical groups. Therefore, it is imperative to concentrate specifically on the process where the first H atom is desorbed from the C atom. For Cu cluster catalysis as depicted in Fig. 3, the most abundant gas-phase Cu₁ and Cu₂ clusters in the growth chamber demonstrate improved barriers of 1.50 eV and 1.57 eV for the initial dehydrogenation of CH₄. Surprisingly, Cu₃ and Cu₄ clusters, with lower content, exhibit even better catalytic performance for the desorption of the first H atom in CH₄, with their barriers significantly reduced to 0.92 eV and 0.77 eV, respectively. We also considered CuH cluster with very stable electronic structure, which exhibits 1.73 eV barrier for the first step dehydrogenation of CH₄, indicating that hydrogenated Cu clusters are still catalytic (Fig. S6). For comparison, Cu(111) surface exhibits barrier of 1.69 eV, indicating that small Cu clusters exhibit more superior catalytic activity for the initial dehydrogenation of CH₄. We investigated the energy barrier for the subsequent dehydrogenation on the most abundant Cu₁ cluster as well. More details correspond to Cu cluster and surface catalysis were given in Sec. 2 of the Supplemental Material.

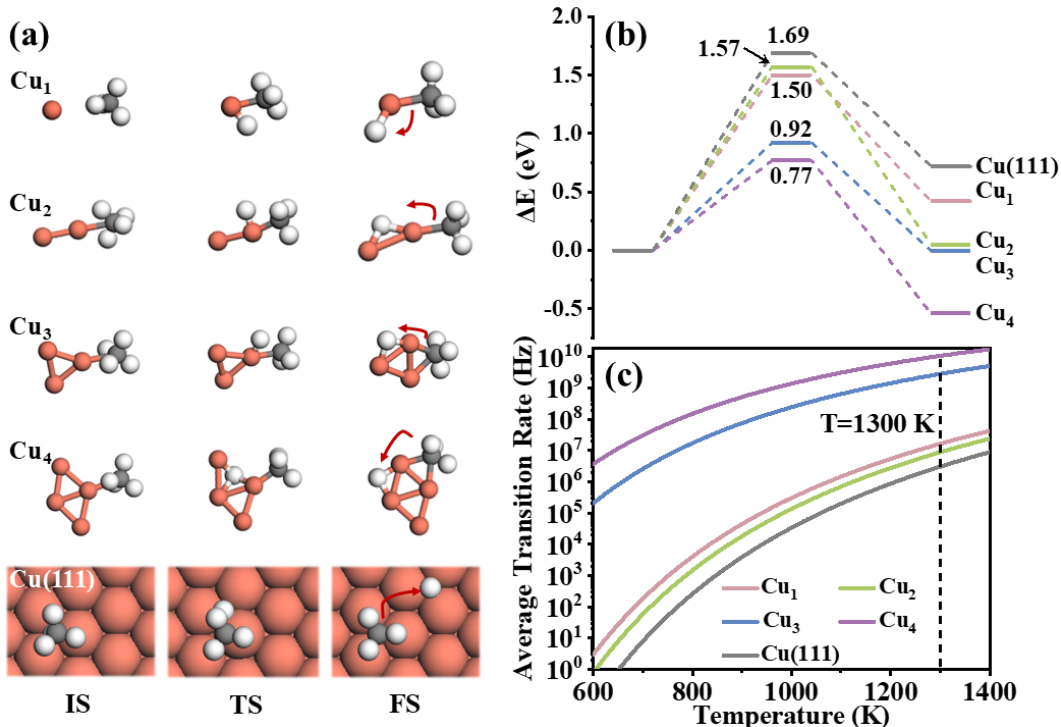


Fig. 3. (a) Atomic structures of initial state (IS), transition state (TS), and final state (FS). (b) Dehydrogenation barriers and (c) Average transition rates of Cu vapor.

The average transition rate for the initial desorption of H atoms from CH₄ can be approximated using the Arrhenius equation:

$$k = A \times e^{-E/k_B T} \quad (9)$$

where the prefactor A is approximately equal to 10^{13} Hz, E denotes the energy barrier. **Fig. 3(c)** illustrates the average transition rates of desorbed hydrogen atoms in Cu₁₋₄ clusters across temperatures ranging from 600 K to 1400 K. At the growth temperature of 1300 K, the atomic vibrational frequency associated with hydrogen atom desorption and migration processes on Cu₁ and Cu₂ clusters reaches 10^7 Hz per second. On Cu₃ and Cu₄ clusters, this frequency can even exceed 10^9 Hz. Such heightened vibrational frequencies strongly suggest that dehydrogenation processes are highly favorable with the assistance of Cu clusters. For comparison, the vibration frequency of Cu(111) surface is only 10^6 Hz, significantly lower than that observed with Cu cluster catalysis. This once again highlights the significant role of isolated gas-phase Cu clusters in the CVD process of graphene growth. Despite the lower abundance of Cu vapor, their impact on gas-phase equilibrium and product control cannot be overlooked.

The assistance role of Cu clusters in the initial dehydrogenation of CH₄ had been elucidated through kinetic analysis. Under growth conditions, there are abundant CH₄ and H₂ in the growth chamber. Subsequently, thermodynamic discussion on the gas-phase equilibrium relationships during graphene growth will be focused. Here, the chemical potential $\mu(T, P)$ and $\chi = P_{CH_4}/P_{H_2}$ were introduced to represent the change in system free energy and CH₄–H₂ gas intake ratio, respectively. According to the NIST-JANAF thermodynamic tables⁴¹ and the previous work⁴⁰, μ_H and μ_C can be derived as following equations:

$$\mu_H(T, P, \chi) = \mu_H(T, P_0) + \frac{1}{2}k_B T \ln \frac{P}{P_0} \frac{1}{1+\chi} \quad (10)$$

$$\mu_C(T, P, \chi) = \Delta g_{CH_4}(T, P_0) - 9.234 + k_B T \ln \frac{P}{P_0} \frac{\chi}{1+\chi} \quad (11)$$

where reference pressure $P_0 = 1 \text{ bar}$. Continuous temperature model was established by fitting the entropy and enthalpy from 800 K to 1400 K of H₂ and CH₄. Based on equations (5), (10), and (11), the symbolic expressions of $\mu_{Cu}(T, P)$, $\mu_H(T, P, \chi)$, and $\mu_C(T, P, \chi)$ regarding temperature T , pressure P and gas intake ratio χ were obtained. Once specific growth conditions were measured from experiment, the values of μ_{Cu} , μ_H , and μ_C can be determined.

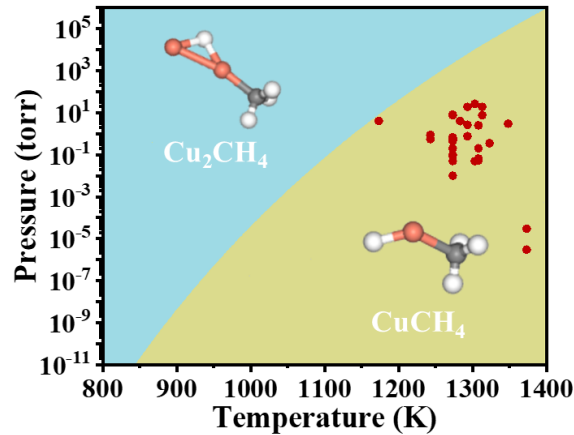


Fig. 4. P–T relationship of stable Cu_xCH_y (x=1,2, y=0~4) clusters. Red dots represent experimental P–T conditions¹¹⁻³⁷.

Further, there are abundant CH₄ and H₂ in the growth chamber under growth conditions. The high surface area and chemical activity of metal clusters enable the formation of complex CuCH ternary clusters, which may act as potential reaction

intermediates under experimental conditions. This prompts important questions about the stability and proportions of these clusters, requiring further thermodynamic analysis to link stability with the P–T conditions of growth. Given the critical role of Cu₁ and Cu₂ in cluster catalysis, probable Cu_xCH_y (x=1,2, y=0~4) cluster structures were carefully considered (see Sec. 3 of the Supplemental Material for more details). The Gibbs free energy of Cu_xCH_y clusters can be expressed by the following formula:

$$G = E_{total} - N_{Cu}\mu_{Cu} - N_C\mu_C - N_H\mu_H \quad (12)$$

For each cluster, its expression of $G(T, P, \chi)$ can be derived by incorporating equations (5), (10), and (11) into (12). Notably, only CuCH₄ and Cu₂CH₄ clusters appear in the phase diagram as depicted in Fig. 4. The CuCH₄ cluster predominantly occupies the phase diagram at higher temperatures and lower pressures. Interestingly, the red dots in the diagram, which represent the P–T conditions observed during experiments, are predominantly located in this region. This suggests that the CuCH₄ cluster is likely the dominant ternary structure following the initial dehydrogenation step.

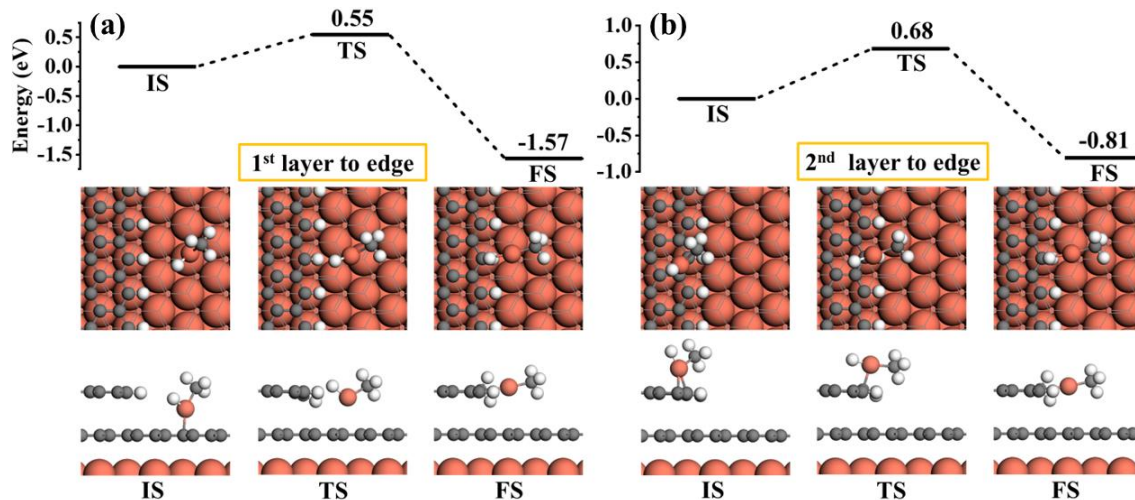


Fig. 5. Migration of CuCH₄ (a) from first layer to edge and (b) from second layer to edge.

After recognizing the catalytic reactivity and stability of clusters, exploring their adsorption behaviors and roles in graphene growth became crucial. There is currently clear experimental evidence indicating that graphene on catalytic substrates such as Cu, Ni, and Ru follows a underneath growth mode, where the second graphene layer nucleates and grows at the bottom of the first graphene layer^{27, 42}. However, this conclusion does not take into account the influence of the continuous supply of catalytic

Cu vapor, where additional Cu vapor clusters may promote the nucleation at the top of existing graphene. According to our previous works⁴³⁻⁴⁶, nucleation kinetics involves defects, impurities, and steps, making the process highly complex. This complexity warrants further in-depth investigation in future studies.

In this work, we propose a hypothesis that nucleation has already occurred in the second layer and there are stable graphene edges. This is similar to the on-top growth mode, where the second layer of graphene grows on the surface of the first layer of graphene⁴⁷⁻⁴⁹. According to our anticipation, the growth of the first graphene layer still relies on the catalytic effect of Cu(111) substrate. Upon completion of the first layer, which shields the Cu surface, the importance of Cu clusters increases. This may lead to layer-by-layer growth of graphene. Thus, a model was constructed featuring graphene supported on Cu(111) substrate, consisting of a complete graphene layer with a localized H-terminated zigzag graphene nanoribbon on the second layer. Subsequent investigations focused on the adsorption of the CuCH₄ cluster onto this system:

$$E_{ads} = E_{total} - E_{sub} - E_{cluster} \quad (13)$$

where E_{total} is the total energy of system, E_{sub} and $E_{cluster}$ represent the energy of substrate and cluster, respectively. According to our results as shown in Fig. 5, the adsorption of CuCH₄ cluster is strongest at the H-terminated edge. Once the CuCH₄ cluster settles on the surfaces of the first and second layers of graphene, it can migrate towards the edge with extremely low barriers of 0.55 eV and 0.68 eV, respectively. The energies of final states are lower than the initial states in both migration paths, indicating the stability of adsorption at the edge. A previous related study pointed out that the passivation of the edge by Cu can reduce the barrier for C atoms to incorporate into the edge from 2.5 eV to 0.8 eV⁵⁰. The above kinetics at the edge of graphene nucleus may represent the upper graphene growing mechanism catalyzed by copper clusters after the Cu substrate is fully covered by graphene. It is important to note that, the underneath growth mode is still widely regarded as the most reasonable explanation for graphene growth. The preceding discussion is predicated on the assumption that stable graphene nuclei reside on the surface of graphene monolayer. Controlled seed introduction may enable the growth of graphene bilayer and multilayer architectures, which requires further experimental evidence.

Our findings elucidated the P–T conditions for Cu vapor formation, its role in CH₄ dehydrogenation, and the kinetics of CuCH₄ cluster at the edge of graphene nucleus. Even after the Cu substrate is covered with a layer of graphene, the presence of free Cu vapor in the growth chamber may still keep reactivity, probably leading to localized bilayer structures. In previous experimental reports of the growth of bilayer graphene, it was hypothesized that the upstream Cu substrate first dehydrogenates CH₄, with methyl radicals flowing downstream to participate in growth^{51, 52}. The subsequent dehydrogenation process was attributed to the weak cross layer catalysis of Cu substrate and the complex gas-phase reactions at high concentrations of methyl radicals. There was lack of detailed consideration about the catalytic role of Cu vapor and the correspond surface defects. The study of Cu cluster catalysis deepens the understanding of graphene preparation.

Methods

First-principles calculations were performed by using the Vienna ab initio simulation package (VASP)⁵³. The generalized gradient approximation (GGA) using the function expressed by Perdew, Burke and Ernzerhof (PBE) was employed to solve the ion-electron interaction⁵⁴. Empirical DFT-D3 (BJ) correction⁵⁵ was introduced according to the Van der Waals interaction induced by C and H atoms. Spin polarization effects were considered by turning on the switch of ISPIN=2. The kinetic energy cutoff of 400 eV was test to ensure an accurate convergence for wave functions. The convergence criteria of energy and force were set to 10⁻⁵ eV and 0.01 eV/Å, respectively. The dehydrogenation and H migration processes were calculated by the climbing image nudged elastic band (CI-NEB) method⁵⁶. We inserted 5 images between initial state and final state to find transition state. Except for necessary transition state parameters, all other settings were consistent with structural optimization. All the accuracy of our numerical procedure had been carefully tested.

Supporting Information

Additional computational details of Cu cluster formation conditions, CH₄ dehydrogenation, and thermodynamic discussions.

Acknowledgment

The authors acknowledge the financial support provided by the National Key R&D Program of China (2024YFA1409600) and the National Natural Science Foundation of China (Grant No. 12374253, 12074053, 12004064). J. G. thanks the foreign talents in the project (G2022127004L) and discussion with Prof. Z. Yu. The authors also acknowledge Computers supporting from DUT supercomputing center, Shanghai Supercomputer Center and Sugon Supercomputer Center.

Reference

1. Liu, C.; Li, Z.; Qiao, R.; Wang, Q.; Zhang, Z.; Liu, F.; Zhou, Z.; Shang, N.; Fang, H.; Wang, M.; Liu, Z.; Feng, Z.; Cheng, Y.; Wu, H.; Gong, D.; Liu, S.; Zhang, Z.; Zou, D.; Fu, Y.; He, J.; Hong, H.; Wu, M.; Gao, P.; Tan, P.-H.; Wang, X.; Yu, D.; Wang, E.; Wang, Z.-J.; Liu, K., Designed growth of large bilayer graphene with arbitrary twist angles. *Nature Materials* **2022**, *21* (11), 1263-1268.
2. Zhang, J.; Liu, X.; Zhang, M.; Zhang, R.; Ta, H. Q.; Sun, J.; Wang, W.; Zhu, W.; Fang, T.; Jia, K.; Sun, X.; Zhang, X.; Zhu, Y.; Shao, J.; Liu, Y.; Gao, X.; Yang, Q.; Sun, L.; Li, Q.; Liang, F.; Chen, H.; Zheng, L.; Wang, F.; Yin, W.; Wei, X.; Yin, J.; Gemming, T.; Rummeli, M. H.; Liu, H.; Peng, H.; Lin, L.; Liu, Z., Fast synthesis of large-area bilayer graphene film on Cu. *Nature Communications* **2023**, *14* (1), 3199.
3. Amontree, J.; Yan, X.; DiMarco, C. S.; Levesque, P. L.; Adel, T.; Pack, J.; Holbrook, M.; Cupo, C.; Wang, Z.; Sun, D.; Biacchi, A. J.; Wilson-Stokes, C. E.; Watanabe, K.; Taniguchi, T.; Dean, C. R.; Hight Walker, A. R.; Barmak, K.; Martel, R.; Hone, J., Reproducible graphene synthesis by oxygen-free chemical vapour deposition. *Nature* **2024**, *630*, 636-642.
4. Li, X.; Cai, W.; Colombo, L.; Ruoff, R. S., Evolution of Graphene Growth on Ni and Cu by Carbon Isotope Labeling. *Nano Letters* **2009**, *9* (12), 4268-4272.
5. Xu, Z.; Xiao, F. S.; Purnell, S. K.; Alexeev, O.; Kawi, S.; Deutsch, S. E.; Gates, B. C., Size-dependent catalytic activity of supported metal clusters. *Nature* **1994**, *372* (6504), 346-348.
6. Hamilton, J. F.; Baetzold, R. C., Catalysis by Small Metal Clusters. *Science* **1979**, *205* (4412), 1213-1220.
7. Lin, L.; Zhang, J.; Su, H.; Li, J.; Sun, L.; Wang, Z.; Xu, F.; Liu, C.; Lopatin, S.; Zhu, Y.; Jia, K.; Chen, S.; Rui, D.; Sun, J.; Xue, R.; Gao, P.; Kang, N.; Han, Y.; Xu, H. Q.; Cao, Y.; Novoselov, K. S.; Tian, Z.; Ren, B.; Peng, H.; Liu, Z., Towards super-clean graphene. *Nature Communications* **2019**, *10* (1), 1912.
8. Jia, K.; Zhang, J.; Lin, L.; Li, Z.; Gao, J.; Sun, L.; Xue, R.; Li, J.; Kang, N.; Luo, Z.; Rummeli, M. H.; Peng, H.; Liu, Z., Copper-Containing Carbon Feedstock for Growing Superclean Graphene.

Journal of the American Chemical Society **2019**, *141* (19), 7670-7674.

9. Su, C.-Y.; Lu, A.-Y.; Wu, C.-Y.; Li, Y.-T.; Liu, K.-K.; Zhang, W.; Lin, S.-Y.; Juang, Z.-Y.; Zhong, Y.-L.; Chen, F.-R.; Li, L.-J., Direct Formation of Wafer Scale Graphene Thin Layers on Insulating Substrates by Chemical Vapor Deposition. *Nano Letters* **2011**, *11* (9), 3612-3616.
10. Kangawa, Y.; Ito, T.; Taguchi, A.; Shiraishi, K.; Ohachi, T., A new theoretical approach to adsorption-desorption behavior of Ga on GaAs surfaces. *Surface Science* **2001**, *493* (1), 178-181.
11. Liu, N.; Fu, L.; Dai, B.; Yan, K.; Liu, X.; Zhao, R.; Zhang, Y.; Liu, Z., Universal Segregation Growth Approach to Wafer-Size Graphene from Non-Noble Metals. *Nano Letters* **2011**, *11* (1), 297-303.
12. Losurdo, M.; Giangregorio, M. M.; Capezzuto, P.; Bruno, G., Graphene CVD growth on copper and nickel: role of hydrogen in kinetics and structure. *Physical Chemistry Chemical Physics* **2011**, *13* (46), 20836-20843.
13. Li, X.; Cai, W.; An, J.; Kim, S.; Nah, J.; Yang, D.; Piner, R.; Velamakanni, A.; Jung, I.; Tutuc, E.; Banerjee, S. K.; Colombo, L.; Ruoff, R. S., Large-Area Synthesis of High-Quality and Uniform Graphene Films on Copper Foils. *Science* **2009**, *324* (5932), 1312-1314.
14. Bae, S.; Kim, H.; Lee, Y.; Xu, X.; Park, J.-S.; Zheng, Y.; Balakrishnan, J.; Lei, T.; Ri Kim, H.; Song, Y. I.; Kim, Y.-J.; Kim, K. S.; Özyilmaz, B.; Ahn, J.-H.; Hong, B. H.; Iijima, S., Roll-to-roll production of 30-inch graphene films for transparent electrodes. *Nature Nanotechnology* **2010**, *5* (8), 574-578.
15. Lee, S.; Lee, K.; Zhong, Z., Wafer Scale Homogeneous Bilayer Graphene Films by Chemical Vapor Deposition. *Nano Letters* **2010**, *10* (11), 4702-4707.
16. Bhaviripudi, S.; Jia, X.; Dresselhaus, M. S.; Kong, J., Role of Kinetic Factors in Chemical Vapor Deposition Synthesis of Uniform Large Area Graphene Using Copper Catalyst. *Nano Letters* **2010**, *10* (10), 4128-4133.
17. Li, X.; Magnuson, C. W.; Venugopal, A.; An, J.; Suk, J. W.; Han, B.; Borysiak, M.; Cai, W.; Velamakanni, A.; Zhu, Y.; Fu, L.; Vogel, E. M.; Voelkl, E.; Colombo, L.; Ruoff, R. S., Graphene Films with Large Domain Size by a Two-Step Chemical Vapor Deposition Process. *Nano Letters* **2010**, *10* (11), 4328-4334.
18. Li, X.; Magnuson, C. W.; Venugopal, A.; Tromp, R. M.; Hannon, J. B.; Vogel, E. M.; Colombo, L.; Ruoff, R. S., Large-Area Graphene Single Crystals Grown by Low-Pressure Chemical Vapor Deposition of Methane on Copper. *Journal of the American Chemical Society* **2011**, *133* (9), 2816-2819.
19. Zhang, Y.; Zhang, L.; Kim, P.; Ge, M.; Li, Z.; Zhou, C., Vapor Trapping Growth of Single-Crystalline Graphene Flowers: Synthesis, Morphology, and Electronic Properties. *Nano Letters* **2012**, *12* (6), 2810-2816.
20. Vlassioux, I.; Fulvio, P.; Meyer, H.; Lavrik, N.; Dai, S.; Datskos, P.; Smirnov, S., Large scale atmospheric pressure chemical vapor deposition of graphene. *Carbon* **2013**, *54*, 58-67.
21. Kobayashi, T.; Bando, M.; Kimura, N.; Shimizu, K.; Kadono, K.; Umezu, N.; Miyahara, K.; Hayazaki, S.; Nagai, S.; Mizuguchi, Y.; Murakami, Y.; Hobara, D., Production of a 100-m-long high-quality graphene transparent conductive film by roll-to-roll chemical vapor deposition and transfer process. *Applied Physics Letters* **2013**, *102* (2).
22. Ryu, J.; Kim, Y.; Won, D.; Kim, N.; Park, J. S.; Lee, E.-K.; Cho, D.; Cho, S.-P.; Kim, S. J.; Ryu, G. H.; Shin, H.-A. S.; Lee, Z.; Hong, B. H.; Cho, S., Fast Synthesis of High-Performance Graphene Films

- by Hydrogen-Free Rapid Thermal Chemical Vapor Deposition. *ACS Nano* **2014**, *8* (1), 950-956.
23. Polsen, E. S.; McNerny, D. Q.; Viswanath, B.; Pattinson, S. W.; John Hart, A., High-speed roll-to-roll manufacturing of graphene using a concentric tube CVD reactor. *Scientific Reports* **2015**, *5* (1), 10257.
24. Deng, B.; Hsu, P.-C.; Chen, G.; Chandrashekar, B. N.; Liao, L.; Ayitimuda, Z.; Wu, J.; Guo, Y.; Lin, L.; Zhou, Y.; Aisijiang, M.; Xie, Q.; Cui, Y.; Liu, Z.; Peng, H., Roll-to-Roll Encapsulation of Metal Nanowires between Graphene and Plastic Substrate for High-Performance Flexible Transparent Electrodes. *Nano Letters* **2015**, *15* (6), 4206-4213.
25. Bointon, T. H.; Barnes, M. D.; Russo, S.; Craciun, M. F., High Quality Monolayer Graphene Synthesized by Resistive Heating Cold Wall Chemical Vapor Deposition. *Advanced Materials* **2015**, *27* (28), 4200-4206.
26. Vlasiouk, I.; Regmi, M.; Fulvio, P.; Dai, S.; Datskos, P.; Eres, G.; Smirnov, S., Role of Hydrogen in Chemical Vapor Deposition Growth of Large Single-Crystal Graphene. *ACS Nano* **2011**, *5* (7), 6069-6076.
27. Li, Q.; Chou, H.; Zhong, J.-H.; Liu, J.-Y.; Dolocan, A.; Zhang, J.; Zhou, Y.; Ruoff, R. S.; Chen, S.; Cai, W., Growth of Adlayer Graphene on Cu Studied by Carbon Isotope Labeling. *Nano Letters* **2013**, *13* (2), 486-490.
28. Lee, D.; Kwon, G. D.; Kim, J. H.; Moyen, E.; Lee, Y. H.; Baik, S.; Pribat, D., Significant enhancement of the electrical transport properties of graphene films by controlling the surface roughness of Cu foils before and during chemical vapor deposition. *Nanoscale* **2014**, *6* (21), 12943-12951.
29. Brown, L.; Lochocki, E. B.; Avila, J.; Kim, C.-J.; Ogawa, Y.; Havener, R. W.; Kim, D.-K.; Monkman, E. J.; Shai, D. E.; Wei, H. I.; Levendorf, M. P.; Asensio, M.; Shen, K. M.; Park, J., Polycrystalline Graphene with Single Crystalline Electronic Structure. *Nano Letters* **2014**, *14* (10), 5706-5711.
30. Yu, H. K.; Balasubramanian, K.; Kim, K.; Lee, J.-L.; Maiti, M.; Ropers, C.; Krieg, J.; Kern, K.; Wodtke, A. M., Chemical Vapor Deposition of Graphene on a "Peeled-Off" Epitaxial Cu(111) Foil: A Simple Approach to Improved Properties. *ACS Nano* **2014**, *8* (8), 8636-8643.
31. Fang, W.; Hsu, A. L.; Song, Y.; Birdwell, A. G.; Amani, M.; Dubey, M.; Dresselhaus, M. S.; Palacios, T.; Kong, J., Asymmetric Growth of Bilayer Graphene on Copper Enclosures Using Low-Pressure Chemical Vapor Deposition. *ACS Nano* **2014**, *8* (6), 6491-6499.
32. Lin, L.; Sun, L.; Zhang, J.; Sun, J.; Koh, A. L.; Peng, H.; Liu, Z., Rapid Growth of Large Single-Crystalline Graphene via Second Passivation and Multistage Carbon Supply. *Advanced Materials* **2016**, *28* (23), 4671-4677.
33. Yoo, M. S.; Lee, H. C.; Lee, S.; Lee, S. B.; Lee, N.-S.; Cho, K., Chemical Vapor Deposition of Bernal-Stacked Graphene on a Cu Surface by Breaking the Carbon Solubility Symmetry in Cu Foils. *Advanced Materials* **2017**, *29* (32), 1700753.
34. Jo, I.; Park, S.; Kim, D.; Moon, J. S.; Park, W. B.; Kim, T. H.; Kang, J. H.; Lee, W.; Kim, Y.; Lee, D. N.; Cho, S.-P.; Choi, H.; Kang, I.; Park, J. H.; Lee, J. S.; Hong, B. H., Tension-controlled single-crystallization of copper foils for roll-to-roll synthesis of high-quality graphene films. *2D Materials* **2018**, *5* (2), 024002.
35. Convertino, D.; Fabbri, F.; Mishra, N.; Mainardi, M.; Cappello, V.; Testa, G.; Capsoni, S.; Albertazzi, L.; Luin, S.; Marchetti, L.; Coletti, C., Graphene Promotes Axon Elongation through Local

- Stall of Nerve Growth Factor Signaling Endosomes. *Nano Letters* **2020**, *20* (5), 3633-3641.
36. Li, J.; Chen, M.; Samad, A.; Dong, H.; Ray, A.; Zhang, J.; Jiang, X.; Schwingschlögl, U.; Domke, J.; Chen, C.; Han, Y.; Fritz, T.; Ruoff, R. S.; Tian, B.; Zhang, X., Wafer-scale single-crystal monolayer graphene grown on sapphire substrate. *Nature Materials* **2022**, *21* (7), 740-747.
37. Sun, L.; Chen, B.; Wang, W.; Li, Y.; Zeng, X.; Liu, H.; Liang, Y.; Zhao, Z.; Cai, A.; Zhang, R.; Zhu, Y.; Wang, Y.; Song, Y.; Ding, Q.; Gao, X.; Peng, H.; Li, Z.; Lin, L.; Liu, Z., Toward Epitaxial Growth of Misorientation-Free Graphene on Cu(111) Foils. *ACS Nano* **2022**, *16* (1), 285-294.
38. Shen, C.; Jia, Y.; Yan, X.; Zhang, W.; Li, Y.; Qing, F.; Li, X., Effects of Cu contamination on system reliability for graphene synthesis by chemical vapor deposition method. *Carbon* **2018**, *127*, 676-680.
39. Lisi, N.; Dikonimos, T.; Buonocore, F.; Pittori, M.; Mazzaro, R.; Rizzoli, R.; Marras, S.; Capasso, A., Contamination-free graphene by chemical vapor deposition in quartz furnaces. *Scientific Reports* **2017**, *7* (1), 9927.
40. Zhang, W.; Wu, P.; Li, Z.; Yang, J., First-Principles Thermodynamics of Graphene Growth on Cu Surfaces. *The Journal of Physical Chemistry C* **2011**, *115* (36), 17782-17787.
41. Malcolm W. Chase, Jr., *NIST-JANAF thermochemical tables*. Fourth edition. Washington, DC : American Chemical Society ; New York : American Institute of Physics for the National Institute of Standards and Technology, 1998.: 1998.
42. Shen, C.; Wang, B.; Chen, Y.; Stehle, R. C.; Zheng, B.; Qing, F.; Niu, X.; Li, X., Unconventional Reaction Phase Diagram for the Penetration Etching/Growth of Graphene Adlayers. *Chemistry of Materials* **2021**, *33* (24), 9698-9707.
43. Gao, J.; Yip, J.; Zhao, J.; Yakobson, B. I.; Ding, F., Graphene Nucleation on Transition Metal Surface: Structure Transformation and Role of the Metal Step Edge. *Journal of the American Chemical Society* **2011**, *133* (13), 5009-5015.
44. Gao, J.; Yuan, Q.; Hu, H.; Zhao, J.; Ding, F., Formation of Carbon Clusters in the Initial Stage of Chemical Vapor Deposition Graphene Growth on Ni(111) Surface. *The Journal of Physical Chemistry C* **2011**, *115* (36), 17695-17703.
45. Yuan, Q.; Gao, J.; Shu, H.; Zhao, J.; Chen, X.; Ding, F., Magic Carbon Clusters in the Chemical Vapor Deposition Growth of Graphene. *Journal of the American Chemical Society* **2012**, *134* (6), 2970-2975.
46. Gao, J.; Ding, F., The Structure and Stability of Magic Carbon Clusters Observed in Graphene Chemical Vapor Deposition Growth on Ru(0001) and Rh(111) Surfaces. *Angewandte Chemie International Edition* **2014**, *53* (51), 14031-14035.
47. Robertson, A. W.; Warner, J. H., Hexagonal Single Crystal Domains of Few-Layer Graphene on Copper Foils. *Nano Letters* **2011**, *11* (3), 1182-1189.
48. Wang, Z.-J.; Dong, J.; Cui, Y.; Eres, G.; Timpe, O.; Fu, Q.; Ding, F.; Schloegl, R.; Willinger, M.-G., Stacking sequence and interlayer coupling in few-layer graphene revealed by in situ imaging. *Nature Communications* **2016**, *7* (1), 13256.
49. Huang, W.; Liu, Z.-F.; Yang, Z.-Y., Top or underneath? Revealing the structure of multilayer graphene domains with atomic force microscopy and theoretical analysis. *Carbon* **2016**, *99*, 131-137.
50. Shu, H.; Chen, X.; Tao, X.; Ding, F., Edge Structural Stability and Kinetics of Graphene Chemical Vapor Deposition Growth. *ACS Nano* **2012**, *6* (4), 3243-3250.

51. Yan, K.; Peng, H.; Zhou, Y.; Li, H.; Liu, Z., Formation of Bilayer Bernal Graphene: Layer-by-Layer Epitaxy via Chemical Vapor Deposition. *Nano Letters* **2011**, *11* (3), 1106-1110.
52. Liu, L.; Zhou, H.; Cheng, R.; Yu, W. J.; Liu, Y.; Chen, Y.; Shaw, J.; Zhong, X.; Huang, Y.; Duan, X., High-Yield Chemical Vapor Deposition Growth of High-Quality Large-Area AB-Stacked Bilayer Graphene. *ACS Nano* **2012**, *6* (9), 8241-8249.
53. Kresse, G.; Furthmüller, J., Efficiency of ab-initio total energy calculations for metals and semiconductors using a plane-wave basis set. *Computational Materials Science* **1996**, *6* (1), 15-50.
54. Perdew, J. P.; Burke, K.; Ernzerhof, M., Generalized Gradient Approximation Made Simple. *Physical Review Letters* **1996**, *77* (18), 3865-3868.
55. Grimme, S.; Ehrlich, S.; Goerigk, L., Effect of the damping function in dispersion corrected density functional theory. *Journal of Computational Chemistry* **2011**, *32* (7), 1456-1465.
56. Henkelman, G.; Uberuaga, B. P.; Jónsson, H., A climbing image nudged elastic band method for finding saddle points and minimum energy paths. *The Journal of Chemical Physics* **2000**, *113* (22), 9901-9904.

Copper Vapor Catalyzing Role in the Growth of Graphene

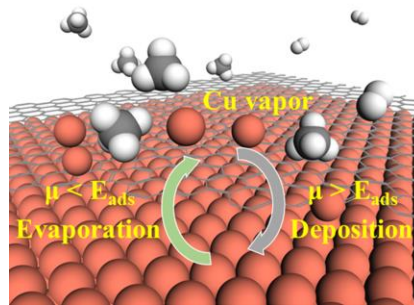
Yuan Chang^{a§}, Shiji Li^{a§}, Tianyu He^a, Hongsheng Liu^a, Junfeng Gao^{a,b*}

^a *State Key Laboratory of Structural Analysis for Industrial Equipment, Dalian University of Technology, Dalian, 116024, China*

^b *Suzhou Laboratory, Suzhou, 215123, China*

*Email: gaojf@dlut.edu.cn

§ Y. C. and S. L. contributed equally to this work



ToC figure.